



ELSEVIER

29 June 1995

PHYSICS LETTERS B

Physics Letters B 353 (1995) 402–412

## A measurement of the $\Lambda_b^0$ lifetime

OPAL Collaboration

R. Akers<sup>p</sup>, G. Alexander<sup>w</sup>, J. Allison<sup>p</sup>, N. Altekamp<sup>e</sup>, K. Ametewee<sup>y</sup>, K.J. Anderson<sup>i</sup>, S. Anderson<sup>l</sup>, S. Arcelli<sup>b</sup>, S. Asai<sup>x</sup>, D. Axen<sup>ac</sup>, G. Azuelos<sup>r,1</sup>, A.H. Ball<sup>q</sup>, E. Barberio<sup>z</sup>, R.J. Barlow<sup>p</sup>, R. Bartoldus<sup>c</sup>, J.R. Batley<sup>e</sup>, G. Beaudoine<sup>r</sup>, S. Bethke<sup>n</sup>, A. Beck<sup>w</sup>, G.A. Beck<sup>m</sup>, C. Beeston<sup>p</sup>, T. Behnke<sup>aa</sup>, K.W. Bell<sup>t</sup>, G. Bella<sup>w</sup>, S. Bentvelsen<sup>h</sup>, P. Berlich<sup>j</sup>, J. Bechtluft<sup>n</sup>, O. Biebel<sup>n</sup>, I.J. Bloodworth<sup>a</sup>, P. Bock<sup>k</sup>, H.M. Bosch<sup>k</sup>, M. Boutemeur<sup>r</sup>, S. Braibant<sup>l</sup>, P. Bright-Thomas<sup>y</sup>, R.M. Brown<sup>t</sup>, A. Buijs<sup>h</sup>, H.J. Burckhart<sup>h</sup>, R. Bürgin<sup>j</sup>, C. Burgard<sup>aa</sup>, P. Capiluppi<sup>b</sup>, R.K. Carnegie<sup>f</sup>, A.A. Carter<sup>m</sup>, J.R. Carter<sup>e</sup>, C.Y. Chang<sup>q</sup>, C. Charlesworth<sup>f</sup>, D.G. Charlton<sup>a,2</sup>, S.L. Chu<sup>d</sup>, P.E.L. Clarke<sup>o</sup>, J.C. Clayton<sup>a</sup>, S.G. Clowes<sup>p</sup>, I. Cohen<sup>w</sup>, J.E. Conboy<sup>o</sup>, O.C. Cooke<sup>p</sup>, M. Cuffiani<sup>b</sup>, S. Dado<sup>v</sup>, C. Dallapiccola<sup>q</sup>, G.M. Dallavalle<sup>b</sup>, C. Darling<sup>ac</sup>, S. De Jong<sup>l</sup>, L.A. del Pozo<sup>h</sup>, H. Deng<sup>q</sup>, M.S. Dixit<sup>g</sup>, E. do Couto e Silva<sup>l</sup>, J.E. Duboscq<sup>h</sup>, E. Duchovni<sup>z</sup>, G. Duckeck<sup>h</sup>, I.P. Duerdoth<sup>p</sup>, U.C. Dunwoody<sup>h</sup>, J.E.G. Edwards<sup>p</sup>, P.G. Estabrooks<sup>f</sup>, H.G. Evans<sup>i</sup>, F. Fabbri<sup>b</sup>, B. Fabbro<sup>u</sup>, M. Fanti<sup>b</sup>, P. Fath<sup>k</sup>, F. Fiedler<sup>l</sup>, M. Fierro<sup>b</sup>, M. Fincke-Keeler<sup>ab</sup>, H.M. Fischer<sup>c</sup>, R. Folman<sup>z</sup>, D.G. Fong<sup>q</sup>, M. Foucher<sup>q</sup>, H. Fukui<sup>x</sup>, A. Fürties<sup>h</sup>, P. Gagnon<sup>f</sup>, A. Gaidot<sup>u</sup>, J.W. Gary<sup>d</sup>, J. Gascon<sup>r</sup>, N.I. Geddes<sup>t</sup>, C. Geich-Gimbel<sup>c</sup>, S.W. Gensler<sup>i</sup>, F.X. Gentit<sup>u</sup>, T. Gerialis<sup>t</sup>, G. Giacomelli<sup>b</sup>, P. Giacomelli<sup>d</sup>, R. Giacomelli<sup>b</sup>, V. Gibson<sup>e</sup>, W.R. Gibson<sup>m</sup>, J.D. Gillies<sup>t</sup>, J. Goldberg<sup>v</sup>, D.M. Gingrich<sup>ad,1</sup>, M.J. Goodrick<sup>e</sup>, W. Gorn<sup>d</sup>, C. Grandi<sup>b</sup>, E. Gross<sup>z</sup>, G.G. Hanson<sup>l</sup>, M. Hansroul<sup>h</sup>, M. Hapke<sup>m</sup>, C.K. Hargrove<sup>g</sup>, P.A. Hart<sup>i</sup>, C. Hartmann<sup>c</sup>, M. Hauschild<sup>h</sup>, C.M. Hawkes<sup>h</sup>, R. Hawkings<sup>h</sup>, R.J. Hemingway<sup>f</sup>, G. Herten<sup>j</sup>, R.D. Heuer<sup>h</sup>, J.C. Hill<sup>e</sup>, S.J. Hillier<sup>h</sup>, T. Hilse<sup>j</sup>, P.R. Hobson<sup>y</sup>, D. Hochman<sup>z</sup>, R.J. Homer<sup>a</sup>, A.K. Honma<sup>ab,1</sup>, R. Howard<sup>ac</sup>, R.E. Hughes-Jones<sup>p</sup>, D.E. Hutchcroft<sup>e</sup>, P. Igo-Kemenes<sup>k</sup>, D.C. Imrie<sup>y</sup>, A. Jawahery<sup>q</sup>, P.W. Jeffreys<sup>t</sup>, H. Jeremie<sup>r</sup>, M. Jimack<sup>a</sup>, A. Joly<sup>r</sup>, M. Jones<sup>f</sup>, R.W.L. Jones<sup>h</sup>, P. Jovanovic<sup>a</sup>, D. Karlen<sup>f</sup>, J. Kanzaki<sup>x</sup>, K. Kawagoe<sup>x</sup>, T. Kawamoto<sup>x</sup>, R.K. Keeler<sup>ab</sup>, R.G. Kellogg<sup>q</sup>, B.W. Kennedy<sup>t</sup>, B.J. King<sup>h</sup>, J. King<sup>m</sup>, J. Kirk<sup>ac</sup>, S. Kluth<sup>e</sup>, T. Kobayashi<sup>x</sup>, M. Kobel<sup>j</sup>, D.S. Koetke<sup>f</sup>, T.P. Kokott<sup>c</sup>, S. Komamiya<sup>x</sup>, R. Kowalewski<sup>h</sup>, T. Kress<sup>k</sup>, P. Krieger<sup>f</sup>, J. von Krogh<sup>k</sup>, P. Kyberd<sup>m</sup>, G.D. Lafferty<sup>p</sup>, H. Lafoux<sup>h</sup>, R. Lahmann<sup>q</sup>, W.P. Lai<sup>s</sup>, D. Lanske<sup>n</sup>, J. Lauber<sup>h</sup>, J.G. Layter<sup>d</sup>, A.M. Lee<sup>ac</sup>, E. Lefebvre<sup>r</sup>, D. Lellouch<sup>z</sup>, J. Letts<sup>b</sup>, L. Levinson<sup>z</sup>, S.L. Lloyd<sup>m</sup>, F.K. Loebinger<sup>p</sup>, G.D. Long<sup>q</sup>, B. Lorazo<sup>r</sup>, M.J. Losty<sup>g</sup>, X.C. Lou<sup>h</sup>, J. Ludwig<sup>j</sup>, A. Luig<sup>j</sup>, A. Malik<sup>u</sup>, M. Mannelli<sup>h</sup>, S. Marcellini<sup>b</sup>, C. Markus<sup>c</sup>, A.J. Martin<sup>m</sup>, J.P. Martin<sup>r</sup>, T. Mashimo<sup>x</sup>, W. Matthews<sup>y</sup>, P. Mättig<sup>c</sup>, J. McKenna<sup>ac</sup>,

E.A. Mckigney<sup>o</sup>, T.J. McMahon<sup>a</sup>, A.I. McNab<sup>m</sup>, F. Meijers<sup>h</sup>, S. Menke<sup>c</sup>, F.S. Merritt<sup>i</sup>,  
H. Mes<sup>g</sup>, A. Michelini<sup>h</sup>, G. Mikenberg<sup>z</sup>, D.J. Miller<sup>o</sup>, R. Mir<sup>z</sup>, W. Mohr<sup>j</sup>, A. Montanari<sup>b</sup>,  
T. Mori<sup>x</sup>, M. Morii<sup>x</sup>, U. Müller<sup>c</sup>, B. Nellen<sup>c</sup>, B. Nijjhar<sup>p</sup>, S.W. O’Neale<sup>a</sup>, F.G. Oakham<sup>g</sup>,  
F. Odorici<sup>b</sup>, H.O. Ogren<sup>l</sup>, N.J. Oldershaw<sup>p</sup>, C.J. Oram<sup>ab,1</sup>, M.J. Oreglia<sup>i</sup>, S. Orito<sup>x</sup>,  
F. Palmonari<sup>b</sup>, J.P. Pansart<sup>u</sup>, G.N. Patrick<sup>t</sup>, M.J. Pearce<sup>a</sup>, P.D. Phillips<sup>p</sup>, J.E. Pilcher<sup>i</sup>,  
J. Pinfold<sup>ad</sup>, D.E. Plane<sup>h</sup>, P. Poffenberger<sup>ab</sup>, B. Poli<sup>h</sup>, A. Posthaus<sup>c</sup>, T.W. Pritchard<sup>m</sup>,  
H. Przysiezniak<sup>ad</sup>, M.W. Redmond<sup>h</sup>, D.L. Rees<sup>a</sup>, D. Rigby<sup>a</sup>, M.G. Rison<sup>e</sup>, S.A. Robins<sup>m</sup>,  
N. Rodning<sup>ad</sup>, J.M. Roney<sup>ab</sup>, E. Ros<sup>h</sup>, A.M. Rossi<sup>b</sup>, M. Rosvick<sup>ab</sup>, P. Routenburg<sup>ad</sup>,  
Y. Rozen<sup>h</sup>, K. Runge<sup>j</sup>, O. Runolfsson<sup>h</sup>, D.R. Rust<sup>l</sup>, M. Sasaki<sup>x</sup>, C. Sbarra<sup>b</sup>, A.D. Schaile<sup>h</sup>,  
O. Schaile<sup>j</sup>, F. Scharf<sup>c</sup>, P. Scharff-Hansen<sup>h</sup>, P. Schenk<sup>d</sup>, B. Schmitt<sup>c</sup>, M. Schröder<sup>h</sup>,  
H.C. Schultz-Coulon<sup>j</sup>, P. Schütz<sup>c</sup>, M. Schulz<sup>h</sup>, J. Schwiening<sup>c</sup>, W.G. Scott<sup>t</sup>, M. Settles<sup>l</sup>,  
T.G. Shears<sup>p</sup>, B.C. Shen<sup>d</sup>, C.H. Shepherd-Themistocleous<sup>g</sup>, P. Sherwood<sup>o</sup>, G.P. Siropoli<sup>b</sup>,  
A. Skillman<sup>o</sup>, A. Skuja<sup>q</sup>, A.M. Smith<sup>h</sup>, T.J. Smith<sup>ab</sup>, G.A. Snow<sup>q</sup>, R. Sobie<sup>ab</sup>,  
S. Söldner-Rembold<sup>j</sup>, R.W. Springer<sup>ad</sup>, M. Sproston<sup>t</sup>, A. Stahl<sup>c</sup>, M. Starks<sup>l</sup>, C. Stegmann<sup>j</sup>,  
K. Stephens<sup>p</sup>, J. Steuerer<sup>ab</sup>, B. Stockhausen<sup>c</sup>, D. Strom<sup>s</sup>, P. Szymanski<sup>t</sup>, R. Tafirout<sup>r</sup>,  
P. Taras<sup>r</sup>, S. Tarem<sup>z</sup>, M. Tecchio<sup>i</sup>, P. Teixeira-Dias<sup>k</sup>, N. Tesch<sup>c</sup>, M.A. Thomson<sup>h</sup>,  
E. von Törne<sup>c</sup>, S. Towers<sup>f</sup>, M. Tscheulin<sup>j</sup>, T. Tsukamoto<sup>x</sup>, A.S. Turcot<sup>i</sup>,  
M.F. Turner-Watson<sup>h</sup>, P. Utzat<sup>k</sup>, R. Van Kooten<sup>l</sup>, G. Vasseur<sup>u</sup>, P. Vikas<sup>r</sup>, M. Vincker<sup>ab</sup>,  
F. Wäckerle<sup>j</sup>, A. Wagner<sup>aa</sup>, D.L. Wagner<sup>i</sup>, C.P. Ward<sup>e</sup>, D.R. Ward<sup>e</sup>, J.J. Ward<sup>o</sup>,  
P.M. Watkins<sup>a</sup>, A.T. Watson<sup>a</sup>, N.K. Watson<sup>g</sup>, P. Weber<sup>f</sup>, P.S. Wells<sup>h</sup>, N. Wermes<sup>c</sup>,  
B. Wilkens<sup>j</sup>, G.W. Wilson<sup>aa</sup>, J.A. Wilson<sup>a</sup>, T. Wlodek<sup>z</sup>, G. Wolf<sup>z</sup>, S. Wotton<sup>k</sup>, T.R. Wyatt<sup>p</sup>,  
G. Yekutieli<sup>z</sup>, V. Zacek<sup>r</sup>, W. Zeuner<sup>h</sup>, G.T. Zorn<sup>q</sup>

<sup>a</sup> School of Physics and Space Research, University of Birmingham, Birmingham B15 2TT, UK

<sup>b</sup> Dipartimento di Fisica dell’ Università di Bologna and INFN, I-40126 Bologna, Italy

<sup>c</sup> Physikalisches Institut, Universität Bonn, D-53115 Bonn, Germany

<sup>d</sup> Department of Physics, University of California, Riverside CA 92521, USA

<sup>e</sup> Cavendish Laboratory, Cambridge CB3 0HE, UK

<sup>f</sup> Carleton University, Department of Physics, Colonel By Drive, Ottawa, Ontario K1S 5B6, Canada

<sup>g</sup> Centre for Research in Particle Physics, Carleton University, Ottawa, Ontario K1S 5B6, Canada

<sup>h</sup> CERN, European Organisation for Particle Physics, CH-1211 Geneva 23, Switzerland

<sup>i</sup> Enrico Fermi Institute and Department of Physics, University of Chicago, Chicago IL 60637, USA

<sup>j</sup> Fakultät für Physik, Albert Ludwigs Universität, D-79104 Freiburg, Germany

<sup>k</sup> Physikalisches Institut, Universität Heidelberg, D-69120 Heidelberg, Germany

<sup>l</sup> Indiana University, Department of Physics, Swain Hall West 117, Bloomington IN 47405, USA

<sup>m</sup> Queen Mary and Westfield College, University of London, London E1 4NS, UK

<sup>n</sup> Technische Hochschule Aachen, III Physikalisches Institut, Sommerfeldstrasse 26-28, D-52056 Aachen, Germany

<sup>o</sup> University College London, London WC1E 6BT, UK

<sup>p</sup> Department of Physics, Schuster Laboratory, The University, Manchester M13 9PL, UK

<sup>q</sup> Department of Physics, University of Maryland, College Park, MD 20742, USA

<sup>r</sup> Laboratoire de Physique Nucléaire, Université de Montréal, Montréal, Quebec H3C 3J7, Canada

<sup>s</sup> University of Oregon, Department of Physics, Eugene OR 97403, USA

<sup>t</sup> Rutherford Appleton Laboratory, Chilton, Didcot, Oxfordshire OX11 0QX, UK

<sup>u</sup> CEA, DAPNIA/SPP, CE-Saclay, F-91191 Gif-sur-Yvette, France

<sup>v</sup> Department of Physics, Technion-Israel Institute of Technology, Haifa 32000, Israel

<sup>w</sup> Department of Physics and Astronomy, Tel Aviv University, Tel Aviv 69978, Israel

<sup>x</sup> International Centre for Elementary Particle Physics and Department of Physics, University of Tokyo, Tokyo 113, Japan  
and Kobe University, Kobe 657, Japan

<sup>y</sup> Brunel University, Uxbridge, Middlesex UB8 3PH, UK

<sup>z</sup> Particle Physics Department, Weizmann Institute of Science, Rehovot 76100, Israel

<sup>aa</sup> Universität Hamburg/DESY, II Institut für Experimental Physik, Notkestrasse 85, D-22607 Hamburg, Germany

<sup>ab</sup> University of Victoria, Department of Physics, P O Box 3055, Victoria BC V8W 3P6, Canada

<sup>ac</sup> University of British Columbia, Department of Physics, Vancouver BC V6T 1Z1, Canada

<sup>ad</sup> University of Alberta, Department of Physics, Edmonton AB T6G 2J1, Canada

<sup>ae</sup> Duke University, Department of Physics, Durham, NC 27708-0305, USA

Received 25 April 1995

Editor: K. Winter

## Abstract

The lifetime of the  $\Lambda_b^0$  baryon has been measured using 3.6 million hadronic  $Z^0$  decays recorded by the OPAL detector at LEP from 1990 to 1994. A sample of  $\Lambda_b^0$  decays is obtained using partially reconstructed semileptonic decays involving  $\Lambda_c^+ \ell^-$  combinations, where the  $\Lambda_c^+$  is reconstructed from its decay to a  $pK^- \pi^+$  final state. From the  $69 \pm 13$   $\Lambda_c^+ \ell^-$  combinations attributed to  $\Lambda_b^0$  decays in this data sample, we measure  $\tau(\Lambda_b^0) = 1.14_{-0.19}^{+0.22} \pm 0.07$  ps, where the errors are statistical and systematic, respectively.

## 1. Introduction

The lifetimes of b-flavored hadrons are determined both by the weak charged current couplings  $V_{cb}$  and  $V_{ub}$  and by the dynamics of the b-hadron decay. Although b-flavored baryons and mesons can each decay via straightforward spectator processes or through the flavor annihilation mechanism (for example W-exchange), the contribution of the latter is less for meson decays relative to baryon decays due to helicity suppression. Therefore one might naively expect b-baryon lifetimes to be shorter than b-meson lifetimes. This expectation is supported by a recent theoretical estimation [1] where the ratio of lifetimes  $\tau(\Lambda_b^0)/\tau(B^0)$  is predicted to be about 0.9.

In this paper, a measurement of the lifetime of the  $\Lambda_b^0$  baryon is described. The decay channel used is<sup>3</sup>

$$\Lambda_b^0 \rightarrow \Lambda_c^+ \ell^- \bar{\nu} (X)$$

$$\hookrightarrow pK^- \pi^+.$$

The b-baryon lifetime has been measured already at LEP using  $\Lambda$ -lepton correlations [2]. Although  $\Lambda_b^0$  decays are expected to be the dominant contribution,

the  $\Lambda$ -lepton events selected may result from a variety of b-baryon decays. The composition of the  $\Lambda$ -lepton sample will depend on the b-baryon production fractions, semileptonic branching ratios and the fraction of their decays that eventually yield a  $\Lambda$ . The lifetime measured is an average one where the b-baryon lifetimes are weighted by their fractions in the final sample. It is therefore interesting to study  $\Lambda_c$ -lepton correlations which provide a purer sample of  $\Lambda_b^0$  decays.

## 2. The OPAL detector

The OPAL detector is described in Ref. [3]. The central tracking system is composed of a precision vertex drift chamber, a large volume jet chamber surrounded by a set of chambers that measure the  $z$ -coordinate ( $z$ -chambers) and, for the majority of the data used in this analysis, a high-precision silicon microvertex detector. These detectors are located inside a solenoidal coil.<sup>4</sup> The detectors outside the solenoid consist of a time-of-flight scintillator array and a lead glass electromagnetic calorimeter with a presampler, followed by a hadron calorimeter consisting of the

<sup>1</sup> Also at TRIUMF, Vancouver, Canada V6T 2A3.

<sup>2</sup> Royal Society University Research Fellow.

<sup>3</sup> In this paper, charge conjugate modes are always implied. Also, unless otherwise noted, K and  $\pi$  always refer to charged particles and  $\ell$  is used for either an electron or muon.

<sup>4</sup> The coordinate system is defined such that the  $z$ -axis follows the electron beam direction and the  $x$ - $y$  plane is perpendicular to it with the  $x$ -axis lying approximately horizontally. The polar angle  $\theta$  is defined relative to the  $+z$ -axis, and the azimuthal angle  $\phi$  is defined relative to the  $+x$ -axis.

instrumented return yoke of the magnet and several layers of muon chambers. Charged particles are identified by their specific energy loss,  $dE/dx$ , in the jet chamber. Further information on the performance of the tracking and  $dE/dx$  measurements can be found in Ref. [4].

### 3. $\Lambda_b^0$ candidate selection

This analysis uses data with center-of-mass energies within  $\pm 3$  GeV of the  $Z^0$  mass collected during the 1990–1994 LEP running periods. After applying standard hadronic event selection [5] and detector performance requirements, a sample of 3.6 million events remains. Charged tracks and electromagnetic clusters not associated with a charged track are combined into jets using the scaled invariant mass algorithm with the E0 recombination scheme [6] using  $y_{\text{cut}} = 0.04$ . Tracks arising from identified  $\gamma$  conversions or secondary vertices due to decays of  $\Lambda$  and  $K_s^0$  are excluded in the  $\Lambda_b^0$  selection.

Monte Carlo simulations of inclusive multihadronic  $Z^0$  decays and of the specific decay mode of interest are used to check the selection procedure. These samples were produced using the JETSET 7.3 parton shower Monte Carlo generator [7] with the fragmentation function of Peterson et al. [8] for heavy quarks and then passed through the full OPAL detector simulation package [9]. A special sample of simulated data was generated using a modified JETSET decay routine for b-baryons [10], where it is assumed that the polarization of the b quark is carried by the b-baryon. An additional decay form factor [11] that describes the energy transfer from the b to c flavored baryon was used in the generation of the polarized sample.

#### 3.1. $\Lambda_c^+ \rightarrow pK^-\pi^+$ selection

In this analysis,  $\Lambda_c$  candidates are reconstructed via their decays into  $pK\pi$ . When searching for  $\Lambda_c$  candidates, all combinations of tracks within a single jet with the appropriate charge combination are considered, provided that they satisfy minimal quality requirements.

Particle identification is used to reduce the combinatorial background. To ensure good separation power of the energy loss measurement in the jet chamber,

proton, kaon and pion candidate tracks are required to have a momentum greater than 3, 2 and 1 GeV/c, respectively. For each track in the  $pK\pi$  combination, the measured  $dE/dx$  is compared with that expected for a given mass hypothesis and the probability that they are consistent is required to be greater than 1%. In addition, if the observed energy loss of the proton or kaon candidate is greater than the mean  $dE/dx$  expected for that particle, the  $dE/dx$  probability is required to be greater than 3%. This cut enhances proton-kaon separation and reduces the pion background. The  $dE/dx$  probability of the pion hypothesis for the proton candidate must also be less than 1%. By reducing the misidentification probability of pions as protons, this last requirement substantially reduces the combinatorial background.

In order to improve the mass and decay length resolutions, at least two of the three candidate tracks are required to have good  $\theta$  measurements either from the z-chambers or from a measurement of the radius at which a track exits the end cone of the jet chamber. The  $pK\pi$  combination is required to have an energy greater than 0.2 of the beam energy in order to reduce random track combinations.

To minimize the possibility of mistaking as a  $\Lambda_c$  the decay  $D_s^+ \rightarrow \phi\pi^+$  (where  $\phi \rightarrow K^+K^-$  and a kaon is misidentified as a proton), the invariant mass of the  $pK$  combination, when assigning the kaon mass to the proton candidate has to differ from the nominal  $\phi$  mass [12] by at least 10 MeV/c<sup>2</sup>. This cut removes essentially all of the  $D_s^+ \rightarrow \phi\pi^+$  background.

#### 3.2. $\Lambda_c^+\ell^-$ selection and decay length determination

Once a  $pK\pi$  combination that satisfies the  $\Lambda_c$  candidate selection is found, a search is performed to find a lepton of opposite charge in the same jet. Electron candidates are identified using an artificial neural network based on twelve measured quantities from the electromagnetic calorimeter and the central tracking detector [13]. Electron candidates identified as arising from photon conversions are rejected [14]. Muons are identified by associating central detector tracks with track segments in the muon detectors and requiring a position match in two orthogonal coordinates [14]. Electron and muon candidates are required to have momenta greater than 2 GeV/c and 3 GeV/c respectively. They must also have transverse momentum with

respect to the direction of the associated jet of at least  $0.8 \text{ GeV}/c$ . The lepton candidate track must also be measured precisely by either the silicon vertex detector or the vertex drift chamber.

In order to suppress background, the mass of the  $pK\pi\ell$  combination must be between  $3.8$  and  $5.2 \text{ GeV}/c^2$ , and the momentum of this combination must be at least  $17 \text{ GeV}/c$ . The cosine of the opening angle between the  $pK\pi$  and lepton directions must be greater than  $0.4$ .

Three vertices – the beam spot, the  $\Lambda_b^0$  decay vertex and the  $\Lambda_c^+$  decay vertex – are reconstructed in the  $x$ - $y$  plane. The beam spot is measured using charged tracks with a technique that follows any significant shifts in the beam spot position during a LEP fill [15]. The intrinsic width of the beam in the  $y$  direction is taken to be  $8 \mu\text{m}$ , from considerations of LEP beam optics. The width in the  $x$  direction is measured directly and varies between  $100 \mu\text{m}$  and  $160 \mu\text{m}$ , depending on the LEP optics.

The  $\Lambda_c$  vertex is reconstructed from a fit using the  $pK\pi$  candidate tracks. The  $\Lambda_b^0$  decay vertex is formed by extrapolating the  $pK\pi$  momentum vector from its decay vertex to its intersection with the lepton track. The  $\Lambda_c$  decay length is the distance between these two decay vertices. The  $\Lambda_c$  lifetime was determined from its decay length distribution to be  $0.21 \pm 0.07$  (stat) ps, in agreement with the PDG value of  $0.200_{-0.010}^{+0.011}$  ps [12]. The  $\Lambda_b^0$  decay length is found by fitting the distance between the beam spot and the reconstructed  $\Lambda_b^0$  decay vertex with the constraint that the  $\Lambda_b^0$  flight direction lie along the  $pK\pi\ell$  momentum vector. The two dimensional projections of the  $\Lambda_b^0$  and  $\Lambda_c^+$  decay lengths are converted into three dimensions using the relevant polar angles which are reconstructed using the momenta of the  $pK\pi\ell$  and  $pK\pi$  combinations, respectively. Typical decay lengths are about  $0.2 \text{ cm}$  for  $\Lambda_b^0$  and  $0.06 \text{ cm}$  for  $\Lambda_c$  baryons. The corresponding typical decay length errors are about  $0.03$  and  $0.06 \text{ cm}$ .

Additional criteria are used to ensure that the selected  $pK\pi$  combinations are suitable for precise decay length measurements. In order to ensure that the  $pK\pi$  candidate tracks come from a common vertex, the  $\chi^2$  of the vertex fit is required to be less than 5 (for 1 degree of freedom). The candidate must also have a decay length error of less than  $0.3 \text{ cm}$ . Using the measured decay length and momentum of the  $pK\pi$

combination, the proper decay time of the  $\Lambda_c$  candidate is determined. This is required to be within two standard deviations of the range from zero to four  $\Lambda_c$  mean lifetimes. Finally, the decay length error of the reconstructed  $\Lambda_b^0$  candidate must be less than  $0.2 \text{ cm}$ .

### 3.3. Results of $\Lambda_c^+\ell^-$ selection

The  $pK\pi$  invariant mass distribution for all  $\Lambda_c^+\ell^-$  candidates is shown in Fig. 1. A clear peak is evident at the position of the  $\Lambda_c$  mass. No such peak is observed in the wrong sign ( $\Lambda_c^+\ell^+$ ) sample (see Fig. 1).

An unbinned maximum likelihood fit to the measured  $pK\pi$  invariant mass of the  $\Lambda_c$  candidates is performed. The  $pK\pi$  mass distribution is parameterized as the sum of a linear term, to account for random combinatorial background, and a Gaussian function, which describes the mass peak of the reconstructed  $\Lambda_c$  signal. This fit yields a  $\Lambda_c$  mass of  $2286 \pm 4 \text{ MeV}/c^2$ , in excellent agreement with the nominal value of  $2285.1 \pm 0.6 \text{ MeV}/c^2$  [12], a width  $\sigma = 20 \pm 4 \text{ MeV}/c^2$  and a total of  $69 \pm 13$  candidates. The fitted combinatorial background fraction is  $0.45 \pm 0.06$  for the  $2\sigma$  interval about the fitted  $\Lambda_c$  mass. The probability that a given event comes from combinatorial background is calculated as a function of its  $pK\pi$  invariant mass using the results of the fit to the mass distribution and is used

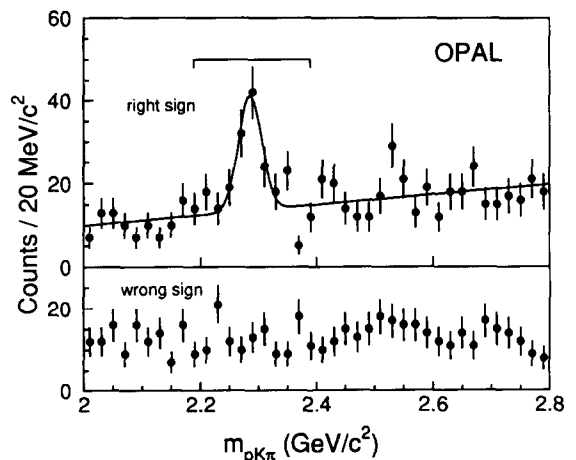


Fig. 1. Top: the  $pK\pi$  invariant mass distribution is shown for  $pK^-\pi^+\ell^-$  combinations along with the fitted curve, which is described in the text. Also indicated is the mass range used in the decay length fit. Bottom: the  $pK\pi$  invariant mass distribution for  $pK^-\pi^+\ell^+$  (wrong sign) candidates is shown.

in the  $\Lambda_b^0$  lifetime fit discussed below. That the event selection and fitting procedure properly estimate the shape and level of the background has been verified by applying the event selection and fitting procedure to samples of simulated data.

### 3.4. Backgrounds to the $\Lambda_c^+\ell^-$ signal

Several potential sources of backgrounds to the  $\Lambda_b^0 \rightarrow \Lambda_c^+\ell^-\bar{\nu}(X)$  signal have been considered. These include decays of other B hadrons that can yield a final state  $\Lambda_c\ell$  combination and charm hadrons that are misidentified as a  $\Lambda_c$  baryon. Other sources are  $\Lambda_c$  baryons combined with a hadron that has been misidentified as a lepton and random associations of  $\Lambda_c$  baryons with genuine leptons.

The events in the  $\Lambda_c$  peak may include properly reconstructed  $\Lambda_c^+\ell^-$  combinations that do not arise from  $\Lambda_b^0$  decay. The following decay modes have been considered:

- (i)  $B_{u,d} \rightarrow \Lambda_c^+\bar{\Xi}_c, \bar{\Xi}_c \rightarrow X\ell^-\bar{\nu}$ ,
- (ii)  $\bar{B}_{u,d,s} \rightarrow \Lambda_c^+X\ell^-\bar{\nu}$ .

The reconstruction efficiencies of these background modes are calculated relative to the signal mode. For the production branching fraction of the signal mode it is assumed that  $f(b \rightarrow \Lambda_b^0) = 0.08 \pm 0.04$  [16]<sup>5</sup> and  $\text{Br}(\Lambda_b^0 \rightarrow \Lambda_c^+\ell^-\bar{\nu}X) = 10 \pm 5\%$ .<sup>6</sup> The latter value is obtained by using the semileptonic branching fraction for B meson decays [12] and the theoretical prediction for  $\tau(\Lambda_b^0)/\tau(B^0)$  of 0.9 [1]. The errors on these quantities are expected to cover all reasonable variations.

To estimate the background from the internal-W decay  $B \rightarrow \Lambda_c^+\bar{\Xi}_c, \bar{\Xi}_c \rightarrow X\ell^-\bar{\nu}$ , the measured inclusive branching ratio  $\text{Br}(B \rightarrow \text{charmed-baryon } X) = 6.4 \pm 1.1\%$  [12] is combined with the assumption that

$$\frac{\text{Br}(B \rightarrow \Lambda_c^+X)}{\text{Br}(B \rightarrow \Lambda_c^+X) + \text{Br}(B \rightarrow \bar{\Lambda}_c^-X)} = 0.5 \pm 0.5.$$

The average semileptonic branching ratio of the charged and neutral  $\Xi_c$  (assuming they are produced with equal rates) is estimated from that of the  $\Lambda_c$ , using the measured lifetimes of these baryons [12], to be  $5.0 \pm 1.9\%$ . With the efficiency included, this mode comprises  $0.7 \pm 0.7\%$  of the signal.

The contribution from the external-W decay,  $\bar{B} \rightarrow \Lambda_c^+X\ell^-\bar{\nu}$ , was estimated using the 90% confidence level limit  $\text{Br}(B \rightarrow \bar{p}e^+\nu X) < 0.16\%$  [17]. It is assumed conservatively that this decay always proceeds through a  $\Lambda_c$  and that B mesons are equally likely to decay into a final state with a proton or a neutron. Thus,  $\text{Br}(B \rightarrow \Lambda_c X\ell\nu) < 0.32\%$  at the 90% confidence level. The analogous decays of  $B_s^0$  mesons are also taken into account by assuming that their branching fraction to  $\Lambda_c X\ell\nu$  is the same as for  $B_{u,d}$  and that  $f(b \rightarrow B_s^0) = 0.12 \pm 0.06$  (see footnote 5). Assuming the probability for a bottom quark to form a  $B^+$  or  $B^0$  meson to be  $0.81 \pm 0.11$  [18], and taking the relative detection efficiency into account, gives an upper limit for this mode corresponding to 3.7% of the signal.

The background from events in which the three  $pK\pi$  candidate tracks come from the same fully reconstructed charm hadron where a pion or a kaon has been misidentified as a proton, or from a partially reconstructed charm hadron, was evaluated using simulated events. For these candidates, the  $pK\pi$  invariant mass distribution around the  $\Lambda_c$  mass is similar to that of the combinatorial background. Such events are therefore considered to be included in the combinatorial background fraction.

The background caused by a  $\Lambda_c$  that has been combined with a hadron that has been misidentified as a lepton can be estimated by fitting the  $pK\pi$  mass spectrum of wrong sign combinations ( $pK^-\pi^+\ell^+$ ), under the assumption that random combinations are equally likely to have right and wrong charge correlations. Using the higher statistics available when  $D^*\ell$  correlations are considered, it is found that this background is less than 1% [13] of that sample and its contribution is therefore neglected. Similarly, no signal is observed when this procedure is repeated with the  $\Lambda_c^+\ell^-$  candidates of this analysis.

The background from random associations of  $\Lambda_c$

<sup>5</sup> The fraction of b quarks that hadronize into  $B_s^0$  and  $\Lambda_b^0$  is estimated as follows. The fraction of b quarks that produce  $B^+$  and  $B^0$  mesons is measured to be  $0.81 \pm 0.11$  [18]. The  $B_s^0$  production fraction is estimated from this to be  $0.12 \pm 0.06$ , where a suppression of 0.3 due to s quark pair production has been assumed. The remaining fraction is conservatively all assigned to  $\Lambda_b^0$  production yielding  $f(b \rightarrow \Lambda_b^0) = 0.08 \pm 0.04$ . The errors assigned to these two estimates are expected to cover all reasonable variations.

<sup>6</sup> For semileptonic branching ratios,  $\ell$  refers to the average of the electron and muon channels.

baryons with genuine leptons was estimated, using simulated data, to contribute less than one event to the sample and has been neglected.

The potential contamination of the signal by decays of b-baryons, other than  $\Lambda_b^0$ , into a  $\Lambda_c$  and a lepton has been investigated. The other principle sources of  $\Lambda_c \ell$  combinations from b-baryons are decays of  $\Xi_b$  and  $\Sigma_b$ . There is some evidence for the  $\Xi_b$  [19], which is expected to decay weakly [20]. Theoretical predictions [20] for the  $\Sigma_b$  mass suggest that it is sufficient to allow strong decays to a  $\Lambda_b^0$ . Accepting this, any non- $\Lambda_b^0$  in the signal must come from  $\Xi_b$  decays. JETSET [7] predicts that 17% of weak b-baryon decays are from  $\Xi_b$ , and the remaining 83% are from  $\Lambda_b^0$ . Semileptonic decays of  $\Xi_b$  baryons to excited charm-strange baryons that subsequently decay to  $\Lambda_c$  or non-resonant decays such as  $\Xi_b \rightarrow \Lambda_c X \ell \nu$  can contribute to the  $\Lambda_c \ell$  sample. The level of these decays has been estimated using the B meson system as a guide. The branching ratio for non-strange B decays to  $X \ell \nu$ , where X is not simply a D or  $D^*$  meson, has been found to be  $3.2 \pm 1.7\%$ . This value is obtained by subtracting  $\text{Br}(B^0 \rightarrow D^- \ell^+ \nu)$  and  $\text{Br}(B^0 \rightarrow D^{*-} \ell^+ \nu)$  from  $\text{Br}(B^0 \rightarrow X \ell^+ \nu)$  using the values from Ref. [12]. The same rate is assumed for the analogous  $\Xi_b$  decays mentioned above and the conservative assumption is made that in these decays a  $\Lambda_c$  is always produced. Given the JETSET predictions for the relative production of the various b-baryons, the above branching ratio estimate and reconstruction efficiencies for the signal mode and the modes under consideration here, only about 1% of the signal could be from the decays of  $\Xi_b$  baryons and as such is neglected.

Background modes for which only an upper limit is available are neglected when deriving the central fitted  $\Lambda_b^0$  lifetime, but their upper limit is taken into account in the determination of the systematic error. Thus, the non-combinatorial background for  $\Lambda_c \ell$  combinations from B meson decay is expected to be  $(0.7^{+3.8}_{-0.7})\%$  of the total  $\Lambda_c \ell$  signal, which corresponds to  $0.5^{+2.6}_{-0.5}$  events. The number of signal candidates from  $\Lambda_b^0 \rightarrow \Lambda_c^+ \ell^- \bar{\nu}(X)$  decays that proceed through the chosen decay chain is found to be

$$N(\Lambda_b^0 \rightarrow \Lambda_c^+ \ell^- \bar{\nu}(X)) = 69 \pm 13.$$

#### 4. The $\Lambda_b^0$ lifetime fit

In order to extract the  $\Lambda_b^0$  lifetime from the measured decay lengths, an unbinned maximum likelihood fit is performed using a likelihood function that accounts for both the signal and background components of the sample. For the component of the likelihood function describing the  $\Lambda_b^0$  signal, the  $\Lambda_b^0$  lifetime must be related to the observed decay lengths using the boost of the  $\Lambda_b^0$ .

Since the neutrino and possibly other particles are not reconstructed, the  $\Lambda_b^0$  momentum,  $p_{\Lambda_b^0}$ , is not known and must be estimated. This is done using the momentum of the  $\Lambda_c \ell$  combination,  $p_{\Lambda_c \ell}$ , and a conversion factor,  $R \equiv p_{\Lambda_c \ell} / p_{\Lambda_b^0}$ , determined from a Monte Carlo simulation. The relationship of the decay time,  $t$ , to the decay length  $L$ , can now be expressed as

$$t = L \cdot R \cdot \frac{m_{\Lambda_b^0}}{p_{\Lambda_c \ell}}, \quad (1)$$

where  $m_{\Lambda_b^0}$  is the  $\Lambda_b^0$  mass. The distribution of the conversion factor  $R$  was determined using simulated data for the  $\Lambda_b^0 \rightarrow \Lambda_c \ell \nu(X)$  signal produced with the JETSET 7.3 Monte Carlo [7], using the fragmentation function of Peterson et al. [8]. The  $R$  distributions were produced for twelve different ranges of the momentum and invariant mass,  $m_{\Lambda_c \ell}$ , of the  $\Lambda_c \ell$  combination. These distributions are used in the lifetime fit to describe the probability that a candidate with a measured  $m_{\Lambda_c \ell}$  and  $p_{\Lambda_c \ell}$  will have a particular value of  $R$ .

The above process of estimating the boost depends on the assumption that the  $\Lambda_c \ell$  combination resulted *directly* from  $\Lambda_b^0$  decay, as only simulated data with this type of event were employed. A decay of the  $\Lambda_b^0$  which can yield a  $\Lambda_c \ell$  combination without a semileptonic decay of the  $\Lambda_b^0$  is  $\Lambda_b^0 \rightarrow \Lambda_c^+ D_s^-$  followed by  $D_s^- \rightarrow X \ell^- \bar{\nu}$ . The lepton in this decay, because it comes from the  $D_s$ , will have a lower mean energy than the leptons in the signal mode. The effect of this background is then an underestimation of the boost which biases the lifetime. The level of this background is determined using the branching ratio of the analogous decay  $B \rightarrow DD_s^+$  [12], where the error has been inflated to 50% of the mean value. When the reconstruction efficiency is included, this source is expected to contribute less than one event to the signal, and is

therefore neglected.

The likelihood function for observing a particular decay length of a  $\Lambda_b^0$  baryon may now be parameterized in terms of the measurement error of the decay length, the  $\Lambda_c \ell$  invariant mass and momentum and the assumed decay time. This function is given by the convolution of three terms: an exponential whose mean is the  $\Lambda_b^0$  lifetime, the boost distribution as given by the values of the observed  $\Lambda_c \ell$  mass and momentum and a Gaussian resolution function whose width is the measured decay length error.

As previously discussed, the dominant sources of *non-combinatorial* backgrounds to the  $\Lambda_c \ell$  signal are all cases in which the  $\Lambda_c$  and lepton both result from  $B^+$  or  $B^0$  decay, either directly or in a subsequent decay. The likelihood function which describes these other sources of background is considered to have the same form as the  $\Lambda_b^0$  signal, except that the lifetime of this sample is fixed to 1.6 ps, which is consistent with the measured average B hadron lifetime [21] and the lifetimes of the  $B^+$  and  $B^0$  hadrons [16]. The level of this background is a fixed fraction of the signal, as was determined in the previous section. The effects of the uncertainty in this value and the lifetime are addressed as a systematic error.

The fit must also account for the combinatorial background present in the  $\Lambda_c \ell$  sample. The functional form used to parameterize this source of background is composed of positive and negative exponentials, each convoluted with the same boost function and Gaussian resolution function as is the signal. The parameters describing the two exponentials and their fractions relative to each other are free parameters in the fit. The exponential shapes are used because at least some of the tracks in these background candidates are often from heavy hadron decays, and as such carry lifetime information. This double exponential shape is motivated by considerations of event topologies that can lead to apparently negative decay lengths, even before resolution effects are considered.

The background which is present in the event sample is taken into account by simultaneously fitting for the signal  $\Lambda_b^0$  decays and background contributions. The expected combinatorial background probability is determined for each candidate using the results of the fit to the  $pK\pi$  invariant mass spectrum. For this fit, only candidates in a region of  $\pm 100 \text{ MeV}/c^2$  about the fitted  $\Lambda_c$  mass are used. From this sample, occur-

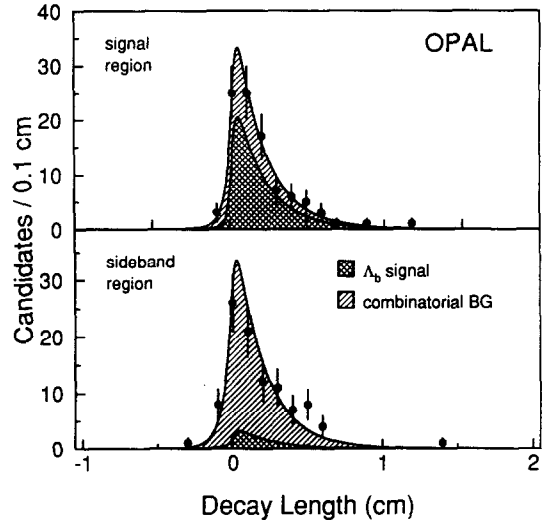


Fig. 2. Top: The decay length distribution of  $pK^-\pi^+\ell^-$  combinations with  $pK\pi$  mass within the  $\Lambda_c$  mass region, defined as  $\pm 30 \text{ MeV}/c^2$  around the fitted  $\Lambda_c$  mass. The area due to the small fraction (0.7%) of background from decays with a true  $\Lambda_c$  and lepton though included in the lifetime fit is too small to see in this plot. Bottom: The decay length distribution of  $pK^-\pi^+\ell^-$  combinations with  $pK\pi$  mass outside the  $\Lambda_c$  mass region. These candidates have  $pK\pi$  mass in the range from  $30 \text{ MeV}/c^2$  to  $100 \text{ MeV}/c^2$  above and below the fitted  $\Lambda_c$  mass. The curves are the result of the fit described in the text.

rences of multiple candidates within a jet have been removed by choosing the candidate with the lowest  $\chi^2$  for the  $pK\pi$  vertex fit. The resulting 193 events are used in the lifetime fit.

Fitting the decay lengths of these candidates gives  $\tau(\Lambda_b^0) = 1.13^{+0.22}_{-0.19} \text{ ps}$ , where the error is statistical only. The decay length distributions are shown in Fig. 2 for those candidates with  $pK\pi$  invariant mass within  $\pm 30 \text{ MeV}/c^2$  of the fitted  $\Lambda_c$  mass, and for those above and below this region. These illustrate the quality of the fit in regions dominated by signal and combinatorial background events respectively. The curves in Fig. 2 represent the sum of the decay length probability distributions for each event. The figures indicate that the fitted functional forms provide a good description of the data for both signal and background. However, it should be noted that the fit is to unbinned data.

## 5. Evaluation of systematic errors

The sources of systematic error considered are due to the level, parameterization and origin of the background, the potential biases from the selection and fitting procedures, the boost estimation method including the effect of possible polarization of the  $\Lambda_b^0$ , the beam spot determination and possible tracking errors.

To determine the effect of the uncertainty in the level of combinatorial background in the  $\Lambda_c^+ \ell^-$  candidates, both the uncertainty in the level of background as determined by the fit to the  $pK\pi$  mass spectrum and the statistical variation of the background under the  $\Lambda_c$  peak have been considered. This is done by repeating the fit to the  $pK\pi$  invariant mass spectrum with the background fraction constrained to be 39% and 51% within a two sigma region about the fitted  $\Lambda_c$  mass, and using the resulting event-by-event background probabilities in the lifetime fit. This yields a variation in the fitted  $\Lambda_b^0$  lifetime of  $\pm 0.03$  ps. The width of the sideband region of the  $pK\pi$  mass spectrum, from which candidates are selected for use in the lifetime fit, has also been varied from  $\pm 75 \text{ MeV}/c^2$  to  $\pm 125 \text{ MeV}/c^2$ , resulting in a change in the fitted lifetime value of  $\pm 0.03$  ps. Various criteria were investigated to ensure that no more than one candidate per jet was used in the lifetime fit. The particular criterion used and any changes in the background fraction that result from this procedure cause the fitted lifetime to vary by at most  $\pm 0.01$  ps. Several alternative background parameterizations have been investigated. For example, terms have been included that allow for significant mismeasurement of tracks and the existence of a zero lifetime component in the combinatorial background. In all cases, these additional terms do not significantly improve the quality of the fit. A fit was also performed replacing the event by event background fraction with one value for the signal region. Sidebands, assumed not to contain any signal events, were used to constrain the background in a simultaneous fit to both regions. The difference in the fitted lifetime when these approaches are used is less than  $+0.01$  ps. The effect of the backgrounds involving  $\Lambda_c \ell$  that are not from the decay of a  $\Lambda_b^0$  baryon, namely from either  $B^+$  or  $B^0$  decays, was also considered. The level of this non-combinatorial background was found above to be  $(0.7^{+3.8}_{-0.7})\%$ . The variation in the level of this background over this range corresponds to an uncer-

tainty of  $^{+0.00}_{-0.01}$  ps. The lifetime of this background is fixed to 1.6 ps for the central result and is varied by  $\pm 0.10$  ps to account for the uncertainty in this value. This variation results in changes to the  $\Lambda_b^0$  lifetime of less than 0.01 ps. The total systematic error from the background parameterization, source and fraction is  $\pm 0.05$  ps.

Tests were performed on several samples of simulated data to check for biases in the selection and fitting methods. The results of these tests on samples of pure signal events are consistent with there being no bias: the ratio of the fitted lifetime to the generated lifetime is  $1.02 \pm 0.03$ . Nonetheless, the measured  $\Lambda_b^0$  lifetime is corrected by this factor and its statistical precision of  $\pm 0.03$  ps is assigned as a systematic error. Similar tests on simulated data including background also show no sign of a bias, albeit with much less statistical precision.

The Monte Carlo data used to estimate the boost were generated using a Peterson fragmentation function, and the range  $\langle x_E \rangle = 0.70 \pm 0.02$  was considered. This produced a change in the measured lifetime of  $\pm 0.01$  ps. The lifetime was also determined by using a mean value for  $R$  in Eq. (1) instead of performing a convolution over the distribution. This produces a change in the measured lifetime of 0.01 ps. The effect on the lifetime of varying the mass of the  $\Lambda_b^0$  about its central value of  $5641 \text{ MeV}/c^2$  by  $\pm 50 \text{ MeV}/c^2$  [12] is  $\pm 0.01$  ps. The presence of missing particles, such as a non-resonant pion produced in the  $\Lambda_b^0$  semileptonic decay or an excited  $\Lambda_c$  state which decays into  $\Lambda_c X$  are estimated to affect the lifetime by at most  $\pm 0.01$  ps.

In the Monte Carlo data used for the boost estimate, the  $\Lambda_b^0$  was assumed to be unpolarized. The polarization was varied between the theoretical limits of 0 and 94% [2] and produced a change of  $+0.06$  ps. The lifetime is therefore corrected by  $+0.03 \pm 0.03$  ps corresponding to a polarization equal to  $(47 \pm 47)\%$ . The effect of the choice of form factor used to describe the energy transfer from the  $\Lambda_b^0$  to the  $\Lambda_c$  has also been investigated. To determine the sensitivity of the fitted lifetime to the choice of the form factor that describes the  $\Lambda_b^0$  decay, alternatives to the form factor of Ref. [11] have been used. Using either no form factor or that proposed in Ref. [22] produces a negligible change in the fitted lifetime.

The average intersection point of the LEP beams in

Table 1  
Summary of systematic errors on the  $\Lambda_b^0$  lifetime

Source	bias (ps)	uncertainty (ps)
background		$\pm 0.05$
possible bias of method	-0.02	$\pm 0.03$
boost		$\pm 0.01$
polarization	+0.03	$\pm 0.03$
beam spot		$\pm 0.01$
alignment errors		$\pm 0.01$
total	+0.01	$\pm 0.07$

OPAL is used as the estimate of the production vertex of the  $\Lambda_b^0$  candidates. The mean coordinates of the beam spot are known to better than  $25 \mu\text{m}$  in the  $x$  direction and  $10 \mu\text{m}$  in  $y$ . The effective r.m.s. spread of the beam is known to a precision of better than  $10 \mu\text{m}$  in both directions. To test the sensitivity of the  $\Lambda_b^0$  lifetime measurement to the assumed position and size of the beam spot, the coordinates of the beam spot are shifted by  $\pm 25 \mu\text{m}$ , and the spreads changed by  $\pm 10 \mu\text{m}$ . The largest observed variation in  $\tau(\Lambda_b^0)$  is  $0.01 \text{ ps}$ , which is assigned as a systematic error.

The effects of alignment and calibration uncertainties on the result are not studied directly but are estimated from a detailed study of 3-prong  $\tau$  decays [15], where the uncertainty in the decay length due to these effects is found to be less than 1.8% for the data taken during 1990 and 1991 and less than 0.4% for later data. This corresponds to an uncertainty on  $\tau(\Lambda_b^0)$  of  $0.01 \text{ ps}$ . The potential for incorrectly estimating the decay length error has been addressed by allowing an additional parameter in the lifetime fit which is a scale factor on the measured decay length error. This parameter is found to be consistent with unity, and its inclusion produces a change in the  $\Lambda_b^0$  lifetime of  $-0.02 \text{ ps}$ .

After applying the correction due to the potential for a bias in the result, and combining the systematic errors in quadrature, we find  $\tau(\Lambda_b^0) = 1.14_{-0.19}^{+0.22} \pm 0.07 \text{ ps}$ , where the first error is statistical and the second is systematic. These systematic errors are summarized in Table 1.

## 6. Conclusion

A sample of  $\Lambda_b^0 \rightarrow \Lambda_c^+ \ell^- \bar{\nu}(X)$  decays has been reconstructed in which the  $\Lambda_c^+$  decays into the  $pK^- \pi^+$  fi-

nal state. From 3.6 million hadronic  $Z^0$  events recorded by OPAL from 1990 to 1994, a total of  $69 \pm 13$  such candidates are attributed to  $\Lambda_b^0$  decays. The  $\Lambda_b^0$  lifetime is found to be

$$\tau(\Lambda_b^0) = 1.14_{-0.19}^{+0.22} \pm 0.07 \text{ ps},$$

where the first error is statistical and the second is systematic. The total relative error corresponds to about 19%. The b-baryon composition of this  $\Lambda_c \ell$  signal is expected to have a higher purity of  $\Lambda_b^0$  decays than analyses that use  $\Lambda \ell$  correlations [2]. It has been estimated that only about 1% of the signal used to determine the above lifetime could have arisen from decays of b-baryons other than a  $\Lambda_b^0$ .

## Acknowledgments

It is a pleasure to thank the SL Division for the efficient operation of the LEP accelerator, the precise information on the absolute energy, and their continuing close cooperation with our experimental group. In addition to the support staff at our own institutions we are pleased to acknowledge the Department of Energy, USA, National Science Foundation, USA, Particle Physics and Astronomy Research Council, UK, Natural Sciences and Engineering Research Council, Canada, Fussesfeld Foundation, Israel Ministry of Science, Israel Science Foundation, administered by the Israel Academy of Science and Humanities, Minerva Gesellschaft, Japanese Ministry of Education, Science and Culture (the Monbusho) and a grant under the Monbusho International Science Research Program, German Israeli Bi-national Science Foundation (GIF), Direction des Sciences de la Matière du Commissariat à l'Énergie Atomique, France, Bundesministerium für Forschung und Technologie, Germany, National Research Council of Canada, A.P. Sloan Foundation and Junta Nacional de Investigação Científica e Tecnológica, Portugal.

## References

- [1] I. Bigi et al., Non-leptonic Decays of Beauty Hadrons – from Phenomenology to Theory, (CERN-TH.7132/94), from the second edition of the book ‘B Decays’, S. Stone (ed.), World Scientific, pp. 132-157;  
I.I. Bigi and N.G. Uraltsev, *Phys. Lett. B* 280 (1992) 271.
- [2] ALEPH Collab., D. Buskulic et al., *Phys. Lett. B* 297 (1992) 449;  
DELPHI Collab., P. Abreu et al., *Phys. Lett. B* 311 (1993) 379;  
OPAL Collab., R. Akers et al., *Phys. Lett. B* 316 (1993) 435.
- [3] OPAL Collab., K. Ahmet et al., *Nucl. Inst. and Meth. A* 305 (1991) 275;  
P.P. Allport et al., *Nucl. Inst. and Meth. A* 324 (1993) 34;  
P.P. Allport et al., *Nucl. Inst. and Meth. A* 346 (1994) 479.
- [4] O. Biebel et al., *Nucl. Inst. and Meth. A* 323 (1992) 169;  
M. Hauschild et al., *Nucl. Inst. and Meth. A* 314 (1992) 74.
- [5] OPAL Collab., G. Alexander et al., *Z. Phys. C* 52 (1991) 175.
- [6] JADE Collab., W. Bartel et al., *Z. Phys. C* 33 (1986) 23;  
JADE Collab., S. Bethke et al., *Phys. Lett. B* 213 (1988) 235.
- [7] T. Sjöstrand, JETSET 7.3 Manual, CERN-TH 6488/92;  
The OPAL parameter optimization is described in  
OPAL Collab., P.D. Acton et al., *Z. Phys. C* 58 (1993) 387.
- [8] C. Peterson et al., *Phys. Rev. D* 27 (1983) 105.
- [9] J. Allison et al., *Nucl. Inst. and Meth. A* 317 (1992) 47.
- [10] A special subroutine for the decays of b-flavored baryons was provided by T. Sjöstrand.
- [11] X.H. Guo and P. Kroll, *Z. Phys. C* 59 (1993) 567.
- [12] Particle Data Group, Review of Particle Properties, *Phys. Rev. D* 50 (1994) 1173.
- [13] OPAL Collab., R. Akers et al., *Phys. Lett. B* 327 (1994) 411.
- [14] OPAL Collab., P.D. Acton et al., *Z. Phys. C* 58 (1993) 523.
- [15] OPAL Collab., P.D. Acton et al., *Z. Phys. C* 59 (1993) 183;  
OPAL Collab., R. Akers et al., *Phys. Lett. B* 338 (1994) 497.
- [16] OPAL Collab., R. Akers et al., Improved Measurements of the  $B^0$  and  $B^+$  Meson Lifetimes, CERN-PPE/95-19, 22 February 1995, submitted to *Z. Phys. C*.
- [17] ARGUS Collab., H. Albrecht et al., *Phys. Lett. B* 249 (1990) 359.
- [18] OPAL Collab., R. Akers et al., A Study of Charm Meson Production in Semileptonic B Decays, CERN-PPE/95-2, 11 January 95, submitted to *Z. Phys. C*.
- [19] DELPHI Collab., P. Abreu et al., Production of strange B-baryons decaying into  $\Xi^{\mp} \ell^{\mp}$  pairs at LEP, CERN-PPE/95-29, 16 March 95, submitted to *Z. Phys. C*.
- [20] W. Kwong and J.L. Rosner, *Phys. Rev. D* 44 (1991) 212.
- [21] OPAL Collab., P.D. Acton et al., *Z. Phys. C* 60 (1993) 217.
- [22] T. Mannel and G. Schuler, *Phys. Lett. B* 279 (1992) 194.